Reprinted from APPLIED OPTICS, Vol. 11, page 667, March 1972

Electromagnetic Scattering by Arbitrarily Oriented Ice Cylinders

Kuo-Nan Liou

The scattering of electromagnetic waves by arbitrarily oriented, infinitely long circular cylinders is solved by following the procedures outlined by van de Hulst. The far-field intensities for two cases of a linearly polarized incident wave are derived. The scattering coefficients involve the Bessel functions of the first kind, the Hankel functions of the second kind, and their first derivatives. Calculations are made for ice cylinders at three wavelengths: 0.7 μ, 3 μ, and 10 μ. The numerical results of intensity coefficients are presented as functions of the observation angle ϕ. A significant cross-polarized component for the scattered field, which vanishes only at normal incidence, is obtained. It is also shown that the numerous interference maxima and minima of the intensity coefficients due to single-particle effects depend on the size parameter x as well as on the oblique incident angle α. Since cylinder-type particles are often observed in ice clouds, the light-scattering calculations performed for a circular cylinder in this paper should be of use in the study of cloud microstructure.

Introduction

While a great many computations have been carried out for light scattering from spherical particles[1-4] based upon the exact solution given by Mie,[5] nothing of a theoretical nature has been set down to predict scattering from large nonspherical particles such as occur in ice clouds. It is very important to understand the angular scattering pattern of ice crystals in order to investigate the radiative transfer through ice clouds. And furthermore, it would be very useful if cloud particles in the liquid and ice phases could be differentiated by using light-scattering measurements.

A rigorous electromagnetic wave solution for hexagonal cylinders, which are often observed in ice clouds,[6] appears likely to be impossible to obtain. As a theoretical approach, we consider in this study the ice crystal that has the shape of a long cylinder with circular cross section. As a result of this assumption, light-scattering calculations for such arbitrarily oriented ice cylinders may then be performed. The primary purpose of this paper is therefore to provide some information on light scattering from ice cylinders.

Scattering of plane waves at normal incidence for a homogeneous dielectric infinite cylinder was solved by Lord Rayleigh[7] in 1917. Since then the solution has been rederived and calculated several times. However, it was not until 1955 that Wait[8] briefly derived a complete solution for oblique incidence on the basis of the procedures developed by Stratton.[9] Little calculation has been accomplished. In this study, we follow most of the notations and procedures outlined by van de Hulst[10] to obtain solutions that are more appropriate for numerical computations.

The scattering geometry for an infinitely long cylinder at oblique incidence is discussed, and the solutions of scattering coefficients and far-field intensities in spherical coordinates are derived. Computations for intensity coefficients are performed for an incident wavelength of 0.7 μ, using a circular radius of 5 μ, and wavelengths of 3 μ and 10 μ with a circular radius of 10 μ. The refractive indices for ice at these wavelengths were taken from a paper by Irvine and Pollack.[11]

Theory

Scattering Geometry

The scattering geometry is shown in Fig. 1. The z axis of the cylindrical coordinates (r,ϕ,z) is placed along the central axis of the cylinder. The angle between the incident ray and the negative z axis is denoted as χ. We further define α as an oblique incident angle which is the complement angle of χ. The x axis is defined in the plane containing the direction of the incident ray and the z axis. This plane defines the angles $\phi = 0$ and $\phi = \pi$. The coordinate r is then contained on the xy plane such that the cylinder occupies the region $r \leq a$, where a is the cross-section radius of the cylinder.

The scattered radiation from an infinitely long cylinder is confined to the surface of a cone. To explain this scattering geometry, let us consider a long cylinder whose diameter is much larger than the incident wavelength, so that the geometric optics may be applied.

The author is with NASA Goddard Space Flight Center, Institute for Space Studies, New York, New York 10025.

Received 20 May 1971.

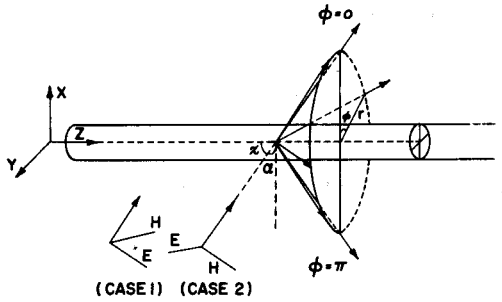

Fig. 1. Geometry for light scattered by an infinitely long cylinder. All symbols are explained in the text.

The rays externally reflected, refracted, or internally reflected on the surface of the cylinder will follow the well-known Snell laws, and consequently the emergent angle and the incident angle are equal. Hence, the scattering of light is confined to the surface of a solid cone which forms an angle α with the xy plane (see Fig. 1).

The scattering angle θ, which is defined as the angle between the directions of the incident wave and the scattered wave, can easily be obtained:

$$\cos\theta = \sin^2\alpha + \cos^2\alpha \cos\phi. \tag{1}$$

We define ϕ as an observation angle to distinguish it from the scattering angle. ϕ and θ become equal only at normal incidence ($\alpha = 0$). In all other cases, the values of θ are always less than that of ϕ. Thus, for an infinite cylinder except at normal incidence, there is no true backscattering.

As for the problem of polarization, we shall consider two simple cases separately. One is when the electric vector $\mathbf{E}$ vibrates parallel to the plane containing the direction of the incident ray and the z axis (case 1), while the other is when the electric vector $\mathbf{E}$ vibrates perpendicular to this plane (case 2). From these two cases, arbitrary elliptically polarized scattered light may then be constructed by means of linear superposition from the two solutions.

Solutions of Scattering Coefficients

In this section we follow most of the notations used by van de Hulst,[10] who outlined the procedures for obtaining the scattering coefficients for light obliquely incident on an infinitely long cylinder of a homogeneous isotropic material. For a periodic electromagnetic field with a circular frequency ω, the well-known Maxwell equations can be expressed as follows:

$$\left.\begin{aligned} \nabla \times \mathbf{H} &= ikm^2\mathbf{E}, \\ \nabla \times \mathbf{E} &= -ik\mathbf{H}, \end{aligned}\right\} \tag{2}$$

where k is the wavenumber in vacuum and m is the complex refractive index of the scattering medium. The electric and magnetic field vectors in a homogeneous medium satisfy the following vector wave equation:

$$\nabla^2\mathbf{A} + k^2m^2\mathbf{A} = 0. \tag{3}$$

Now, if Ψ satisfies the scalar wave equation

$$\nabla^2\Psi + k^2m^2\Psi = 0, \tag{4}$$

it can be proved that vectors $\mathbf{M}_\Psi$ and $\mathbf{N}_\Psi$ in cylindrical coordinates (r,ϕ,z) defined by

$$\left.\begin{aligned} \mathbf{M}_\Psi = \nabla \times (\mathbf{a}_z\Psi) &= \mathbf{a}_r \frac{1}{r}\frac{\partial\Psi}{\partial\phi} - \mathbf{a}_\phi \frac{\partial\Psi}{\partial r}, \\ mk\mathbf{N}_\Psi = \nabla \times \mathbf{M}_\Psi &= \mathbf{a}_r \frac{\partial^2\Psi}{\partial z\partial r} + \mathbf{a}_\phi \frac{1}{r}\frac{\partial^2\Psi}{\partial z\partial\phi} \\ &\quad - \mathbf{a}_z\left[\frac{1}{r}\frac{\partial}{\partial r}\left(r\frac{\partial\Psi}{\partial r}\right) + \frac{1}{r^2}\frac{\partial^2\Psi}{\partial\phi^2}\right], \end{aligned}\right\} \tag{5}$$

satisfy Eq. (3), where $\mathbf{a}_r$, $\mathbf{a}_\phi$, and $\mathbf{a}_z$ are unit vectors.

Suppose that u and v are two orthogonal solutions of Eq. (4), then the Maxwell equations (2) are satisfied by the field vectors defined by

$$\left.\begin{aligned} \mathbf{E} &= \mathbf{M}_v + i\mathbf{N}_u, \\ \mathbf{H} &= m(-\mathbf{M}_u + i\mathbf{N}_v). \end{aligned}\right\} \tag{6}$$

The scalar wave equation (4) in cylindrical coordinates can be expressed as:

$$\frac{1}{r}\frac{\partial}{\partial r}\left(r\frac{\partial\Psi}{\partial r}\right) + \frac{1}{r^2}\frac{\partial^2\Psi}{\partial\phi^2} + \frac{\partial^2\Psi}{\partial z^2} + m^2k^2\Psi = 0. \tag{7}$$

This equation is separable by letting $\Psi = R(r)\Phi(\phi)Z(z)$. Since within a homogeneous, isotropic medium every electromagnetic field may be represented by a linear combination of elementary wavefunctions, then the elementary solutions of Eq. (7) have the following form:

$$\Psi_n = \exp(i\omega t)Z_n(jr)\exp(in\phi)\exp(-ihz), \tag{8}$$

where h is an arbitrary constant, n is an integer, $j = (m^2k^2 - h^2)^{\frac{1}{2}}$, and Z_n is any Bessel function of order n. Since the cylinder is assumed to be infinitely long, the field must be periodic in the z direction. Thus, two solutions u and v in Eq. (6) contain $\cos n\phi$ and $\sin n\phi$, respectively. By virtue of Eqs. (5) and (7), Eq. (6) may then be explicitly expressed as:

$$\left.\begin{aligned} \mathbf{E} &= \mathbf{a}_r\left(-\frac{in}{r}v + \frac{h}{mk}\frac{\partial u}{\partial r}\right) \\ &\quad + \mathbf{a}_\phi\left(-\frac{\partial v}{\partial r} - \frac{inh}{mkr}u\right) + \mathbf{a}_z\left[\frac{i(m^2k^2 - h^2)}{mk}u\right], \\ \mathbf{H} &= \mathbf{a}_r\left(\frac{inm}{r}u + \frac{h}{k}\frac{\partial v}{\partial r}\right) \\ &\quad + \mathbf{a}_\phi\left(m\frac{\partial u}{\partial r} - \frac{inh}{kr}v\right) + \mathbf{a}_z\left[\frac{i(m^2k^2 - h^2)}{k}v\right]. \end{aligned}\right\} \tag{9}$$

Using the well-known addition theorem for Bessel functions (see Stratton[9]) and noting that $x = r\cos\phi$, the incident field (with amplitude unity) can be expressed as:

$$\Psi^i = \exp[i\omega t - ik(x\cos\alpha + z\sin\alpha)] = \sum_n F_nJ_n(lr), \tag{10}$$

where

$$F_n = (-i)^n \exp[i(\omega t + n\phi - hz)],$$
$$h = k\sin\alpha,$$
$$l = k\cos\alpha.$$

It should be noted that Σ_n represents summation over n from $-\infty$ to $+\infty$. For scattered waves, the radial function Z_n is the Hankel function of the second kind $H_n^{(2)}(lr)$ which ensures the proper behavior of the field at infinity. For internal waves, the radial function Z_n is the Bessel function of the first kind $J_n(jr)$, which is selected to ensure that the field is finite at $r = 0$.

Now we shall consider two simple cases separately. First, the electric vector **E** is parallel to the xz plane ($v^i = 0$). This is sometimes called the TM mode. We obtain the two solutions for the scalar wave equation inside and outside the cylinder as follows:

$$\left.\begin{aligned} &r > a, \\ &u^i = \sum_n F_n J_n(lr), \\ &u^s = \sum_n -b_{n_1} F_n H_n^{(2)}(lr), \\ &v^s = \sum_n -a_{n_1} F_n H_n^{(2)}(lr), \\ &r < a, \\ &u^t = \sum_n d_{n_1} F_n J_n(jr), \\ &v^t = \sum_n c_{n_1} F_n J_n(jr), \end{aligned}\right\} \quad (11)$$

where the superscripts i, s, and t represent the incident, scattered, and internal fields, respectively. It should be noted that although $v^i = 0$, v^s and v^t will not be zero due to the oblique incidence. For the second case, the electric vector **E** perpendicular to the xz plane ($u^i = 0$), we obtain (TE mode):

$$\left.\begin{aligned} &r > a, \\ &v^i = \sum_n F_n J_n(lr), \\ &v^s = \sum_n -a_{n_2} F_n H_n^{(2)}(lr), \\ &u^s = \sum_n -b_{n_2} F_n H_n^{(2)}(lr), \\ &r < a, \\ &u^t = \sum_n d_{n_2} F_n J_n(jr), \\ &v^t = \sum_n c_{n_2} F_n J_n(jr). \end{aligned}\right\} \quad (12)$$

It is seen that case 1 and case 2 differ only in the initial conditions $u^i = 0$ or $v^i = 0$.

The boundary conditions require that the tangential components of **E** and **H** be continuous at the interface, i.e.,

$$\left.\begin{aligned} E_\phi{}^i + E_\phi{}^s = E_\phi{}^t, \quad & H_\phi{}^i + H_\phi{}^s = H_\phi{}^t, \\ E_z{}^i + E_z{}^s = E_z{}^t, \quad & H_z{}^i + H_z{}^s = H_z{}^t, \end{aligned}\right\} \text{ at } r = a. \quad (13)$$

By virtue of Eqs. (9) and (11) and Eqs. (9) and (12), we get two sets of four linear equations for coefficients a_n, b_n, c_n, and d_n from Eq. (13). After making some algebraic operations, we obtain the scattering coefficients a_n and b_n as follows:

$$\left.\begin{aligned} b_{n_1} &= P_n \frac{Q_n{}^2 + A_n(\varepsilon_1)B_n(\varepsilon_2)}{Q_n{}^2 + A_n(\varepsilon_1)A_n(\varepsilon_2)}, \\ a_{n_2} &= P_n \frac{Q_n{}^2 + B_n(\varepsilon_1)A_n(\varepsilon_2)}{Q_n{}^2 + A_n(\varepsilon_1)A_n(\varepsilon_2)}, \\ a_{n_1} &= -b_{n_2} = P_n Q_n \frac{A_n(\varepsilon_1) - B_n(\varepsilon_1)}{Q_n{}^2 + A_n(\varepsilon_1)A_n(\varepsilon_2)}, \end{aligned}\right\} \quad (14)$$

where
$$A_n(\varepsilon_{1,2}) = j\frac{H_n^{(2)\prime}(la)}{H_n^{(2)}(la)} - \varepsilon_{1,2}l\frac{J_n'(ja)}{J_n(ja)},$$
$$B_n(\varepsilon_{1,2}) = j\frac{J_n'(la)}{J_n(la)} - \varepsilon_{1,2}l\frac{J_n'(ja)}{J_n(ja)}, \quad \begin{cases}\varepsilon_1 = 1, \\ \varepsilon_2 = m^2,\end{cases}$$
$$P_n = J_n(la)/H_n^{(2)}(la),$$
$$Q_n = inh(l^2 - j^2)/xlj,$$
$$x = ka = 2\pi a/\lambda, \quad \lambda = \text{wavelength}.$$

At this point, the solutions for scattering coefficients are complete. The primes over the Bessel functions of the first kind and the Hankel functions of the second kind denote the differentiation with respect to the whole argument. If we let $\alpha = 0°$ (normal incidence), $a_{n_1} = b_{n_2} = 0$, the scattering coefficients b_{n_1} and a_{n_2} can be reduced to the forms presented by van de Hulst.[10] While the assumption is made that the cylinder is infinitely long, the solutions for scattering coefficients, however, should be applied to a finite cylinder whose length is much larger than its diameter with rather good accuracy. The wavenumber k contained in Eq. (14) can be canceled out, except when it is coupled with the radius a. Thus, b_{n_1}, a_{n_2}, and a_{n_1} are readily adaptable to machine calculations. We should note that these coefficients depend on the refractive index m, the size parameter x, and the oblique incident angle α. In the next section we obtain the expressions for the scattered intensities at far field.

Intensities at Far Field

At far field, the asymptotic form for the Hankel function of the second kind is

$$H_n^{(2)}(lr) \simeq (2/\pi lr)^{\frac{1}{2}} \exp[-ilr + i(2n+1)\pi/4], \quad (lr) \to \infty. \quad (15)$$

From Eqs. (11) and (12), we obtain readily the values of u^s and v^s at a great distance. For case 1, they are (similar discussions hold for case 2; we neglect the details for simplicity):

$$\left.\begin{aligned} u^s &= \left(\frac{2}{\pi lr}\right)^{\frac{1}{2}} \exp[i(\omega t - hz - lr) - i3\pi/4] \sum_n b_{n_1} \cos n\phi, \\ v^s &= \left(\frac{2}{\pi lr}\right)^{\frac{1}{2}} \exp[i(\omega t - hz - lr) - i3\pi/4] \sum_n a_{n_1} \sin n\phi. \end{aligned}\right\} \quad (16)$$

By neglecting terms of the order of $(1/r)$ higher than $(1/r)^{\frac{1}{2}}$, we can express the three components of electric field at a great distance from Eq. (9):

$$\left.\begin{aligned} E_r^s &\simeq -ik \sin\alpha \cos\alpha\, u^s, \\ E_\phi^s &\simeq ik \cos\alpha\, v^s, \\ E_z^s &\simeq ik \cos^2\alpha\, u^s. \end{aligned}\right\} \tag{17}$$

We would like to express the resulting field in spherical coordinates (R,θ,ϕ), where R represents the distance of the propagation of waves. By using the following relationships:

$$\left.\begin{aligned} E_R &= E_r \cos\alpha + E_z \sin\alpha, \\ E_\theta &= -E_r \sin\alpha + E_z \cos\alpha, \end{aligned}\right\} \tag{18}$$

we obtain immediately the electric field in spherical coordinates:

$$\left.\begin{aligned} E_R^s &\simeq 0, \\ E_\theta^s &\simeq ik \cos\alpha \left(\frac{2}{\pi kR}\right)^{\frac{1}{2}} \\ &\quad \times \exp(i\omega t - ikR - i3\pi/4) \sum_n b_{n1} \cos n\phi, \\ E_\phi^s &\simeq ik \cos\alpha \left(\frac{2}{\pi kR}\right)^{\frac{1}{2}} \\ &\quad \times \exp(i\omega t - ikR - i3\pi/4) \sum_n a_{n1} \sin n\phi, \end{aligned}\right\} \tag{19}$$

where $R = r\cos\alpha + z\sin\alpha$. Thus, if light of intensity $I_0(W/m^2)$, which is polarized parallel (case 1) or perpendicular (case 2) to the plane containing the direction of the incident ray and z axis, is incident on the cylinder with an incident angle α, the intensities of the scattered light in any direction are

$$\left.\begin{aligned} I_{11} &= 2i_{11}I_0/\pi kR, \\ I_{12} &= 2i_{12}I_0/\pi kR, \end{aligned}\right\} \quad \text{case 1,} \tag{20}$$

$$\left.\begin{aligned} I_{22} &= 2i_{22}I_0/\pi kR, \\ I_{21} &= 2i_{21}I_0/\pi kR, \end{aligned}\right\} \quad \text{case 2,} \tag{21}$$

where the intensity coefficients are defined as

$$\left.\begin{aligned} i_{11} &= \left|b_{01} + 2\sum_{n=1}^{\infty} b_{n1} \cos n\phi\right|^2, \\ i_{12} &= \left|2\sum_{n=1}^{\infty} a_{n1} \sin n\phi\right|^2, \end{aligned}\right\} \tag{22}$$

$$\left.\begin{aligned} i_{22} &= \left|a_{02} + 2\sum_{n=1}^{\infty} a_{n2} \cos n\phi\right|^2, \\ i_{21} &= \left|2\sum_{n=1}^{\infty} b_{n2} \sin n\phi\right|^2, \end{aligned}\right\} \tag{23}$$

and $$i_{12} = i_{21}.$$

I_{11} and I_{22} are the scattered intensities that lie in the same plane as the incident intensities, while I_{12} and I_{21} are the cross-polarized (or depolarized) scattered intensities that have directions perpendicular to the incident intensities. The intensity coefficients i_{11},i_{12} and i_{22},i_{21} have meaning similar to i_1 and i_2 in the case of the spherical particles. In the next section, we present numerical results for i_{11}, i_{22}, and i_{12} as functions of observation angles ϕ for a given angle α.

Results

The computations for intensity coefficients i_{11}, i_{22}, and i_{12} are rather simple except for the scattering coefficients a_n and b_n, which involve the Bessel functions of the first kind, the Hankel functions of the second kind, and their first derivatives. The Hankel function of the second kind for any argument x is

$$H_n^{(2)}(x) = J_n(x) - iY_n(x), \tag{24}$$

where Y_n is the Bessel function of the second kind. The numerical computations were carried out on an IBM 360/95 computer using a Fortran program. The Bessel functions were evaluated by employing the IBM scientific subroutines which were based on the technique developed by Abramowitz and Stegun.[12]

In this study, three cases have been chosen for light-scattering computations; the first is a cylinder of 5-μ circular radius with an incident wavelength of 0.7 μ, the second and third are cylinders of circular radii of 10 μ with incident wavelengths of 3 μ and 10 μ, respectively. The refractive indices for ice at these three wavelengths were obtained from the values tabulated by Irvine and Pollack,[11] and the calculations were made at 361 observation angles, 0° (0.5°) 180°.

Figure 2 represents the intensity coefficients for light scattered by the cylinder of circular radius 5 μ with an incident wavelength of 0.7 μ. The real part of the refractive index for ice at this visible wavelength is 1.31, with the imaginary part being negligible. The size parameter x in this case is equal to 44.88. The plots are presented in such a way that the scattered intensity coefficients, which change with the incident angle α, can be clearly shown. In the upper part of this figure are the two extreme cases for α of 5° and 85°. One represents near-normal incidence (α = 5°), while the other denotes the incidence almost parallel to the cylinder (α = 85°). It should be noted that when α = 90°, i.e., the incident beam is parallel to the z axis of the cylinder, the values of a_n and b_n are indefinite. This is the case of singularity. Physically this means that the cylinder does not scatter light at all, since an infinitely long cylinder is being considered here. For an incident angle of 5°, the number of maxima and minima fluctuations due to the single-particle effects is approximately equal to the size parameter x. Around an observation angle of 140°, a general maximum indication for i_{11} is seen which is quite similar to the case of Mie spherical particles (rainbow region). For a large oblique incident angle of 85°, the scattering pattern for both i_{11} and i_{22} becomes very simple and nearly symmetrical, with a minimum at an observation angle of 90°. The lower part of Fig. 2 shows the intensity coefficients i_{11} and i_{22} for incident angles α of 45° and 70°. We choose these two angles to show two intermediate scattering patterns. The number of maxima or minima of i_{11} and i_{22} for α of 45° decreases to 27, while for α of 70°, there are only 11. Generally, the values of intensity coefficients seem to decrease with increasing α. Moreover, a pronounced diffraction peak is noted at forward directions for small oblique incident angles of 5° and 45°.

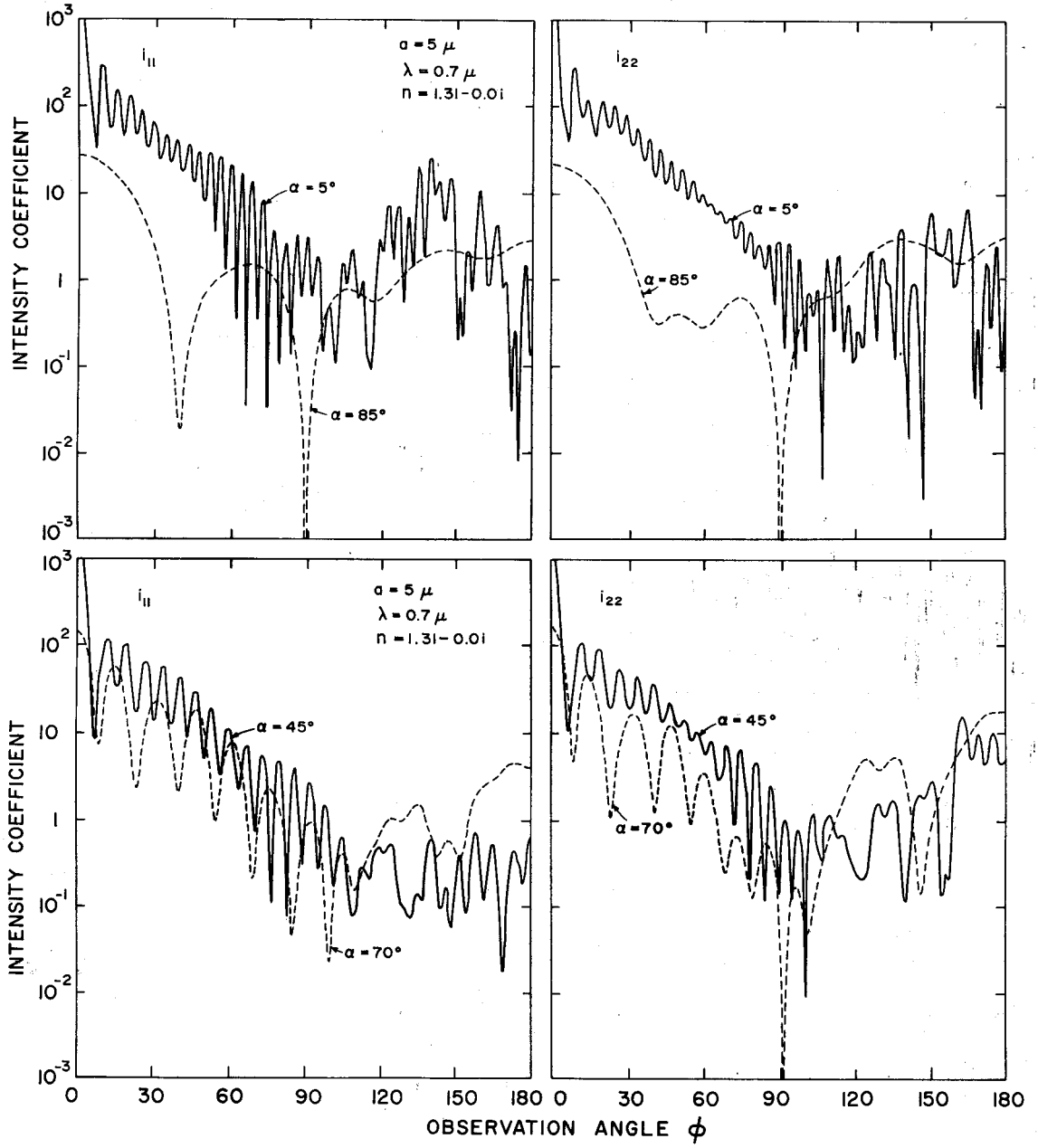

Fig. 2. Intensity coefficients i_{11} (left-hand side) and i_{22} (right-hand side) as functions of observation angle ϕ for light scattered by a cylinder of circular radius a of 5 μ with incident wavelength λ of 0.7 μ. The upper parts are for oblique incident angles α of 5° (*solid line*) and 85° (*dotted line*). The lower parts are for oblique incident angles of 45° (*solid line*) and 70° (*dotted line*).

The cross-polarized intensity coefficient i_{12} for four oblique incident angles is shown in Fig. 3. When α = 5°, values of i_{12} are generally very small, as can be expected, since at normal incidence this cross-component vanishes. The number of maxima and minima again decrease with increasing α. At observation angles ϕ of 0° and 180°, the cross-components i_{12} for these two cases equal zero, i.e., the scattered light retains the same polarization as that of the incident radiation. Compared to Fig. 2, it is seen that i_{12} has values comparable with those of i_{11} and i_{22} except at the very forward observation angles.

Figure 4 shows the intensity coefficients i_{11} and i_{22} for light scattered by an ice cylinder of circular radius 10 μ with an incident wavelength of 10 μ. The size parameter x is equal to 6.28 in this case. The real and imaginary parts of the refractive index are 1.152 and 0.0413, respectively, for a wavelength of 10 μ. Absorption is expected to take place inside the cylinder. Since we consider a long cylinder such that its size is

much larger than the incident wavelength in this study, the light may be considered as consisting of separate localized rays which travel along straight-line paths.[4,10] The absorption depends on the optical path of the rays refracted and those internally reflected several times in the cylinder. The solid and dotted lines and the combinations of the dotted lines and black dots in this figure (and also Figs. 5 and 6) represent oblique incident angles α of 5°, 45°, and 85°, respectively. For α of 5° and 45°, the diffraction peak at the forward direction can be easily seen and since the size parameter is quite small, few maxima and minima are presented. When α is 85°, the patterns for both intensity coefficients i_{11} and i_{22} become nearly symmetrical

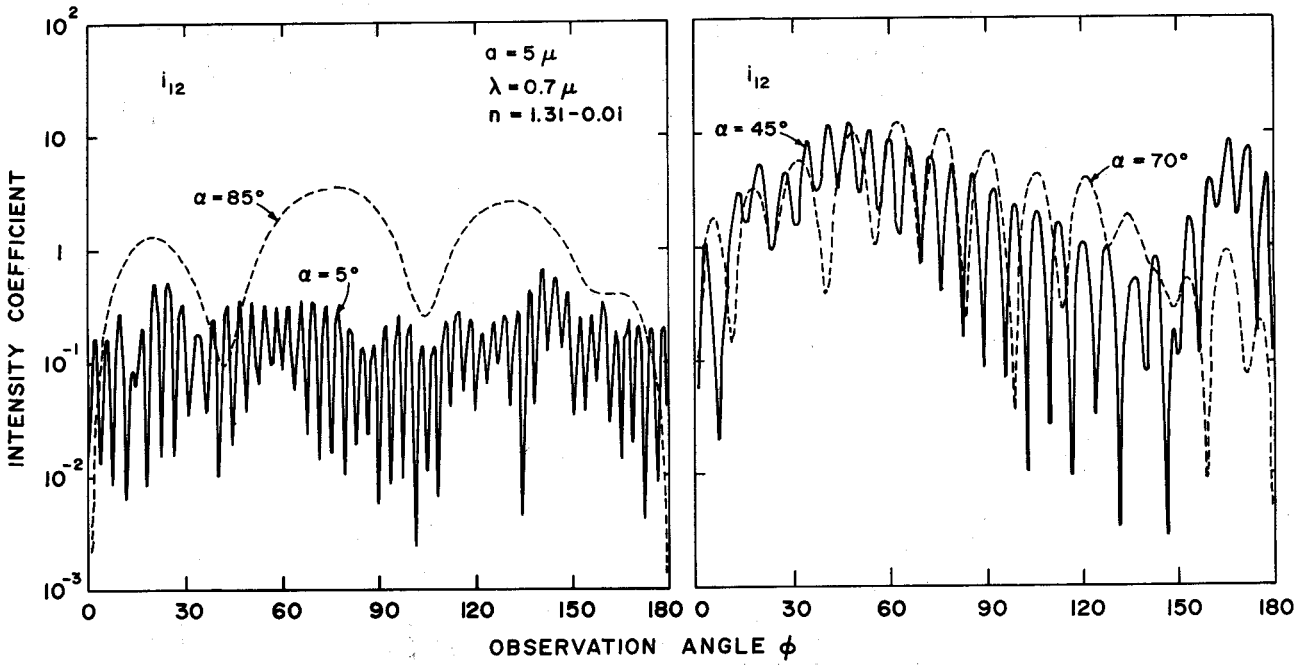

Fig. 3. Same as Fig. 2, but for cross-polarized intensity coefficient i_{12}.

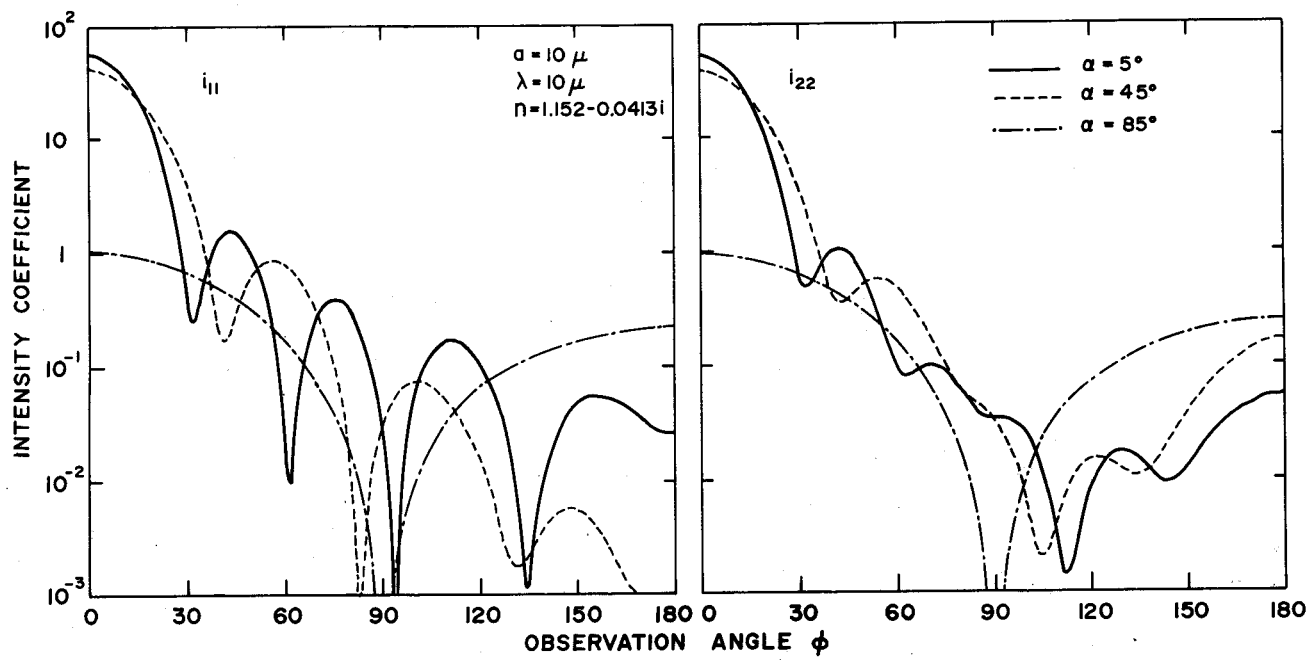

Fig. 4. Intensity coefficients i_{11} (left-hand side) and i_{22} (right-hand side) as functions of observation angle ϕ for light scattered by a cylinder of circular radius a of 10 μ with incident wavelength λ of 10 μ. Solid lines, dotted lines, and combinations of solid lines and dotted lines are for oblique incident angles α of 5°, 45°, and 85°, respectively.

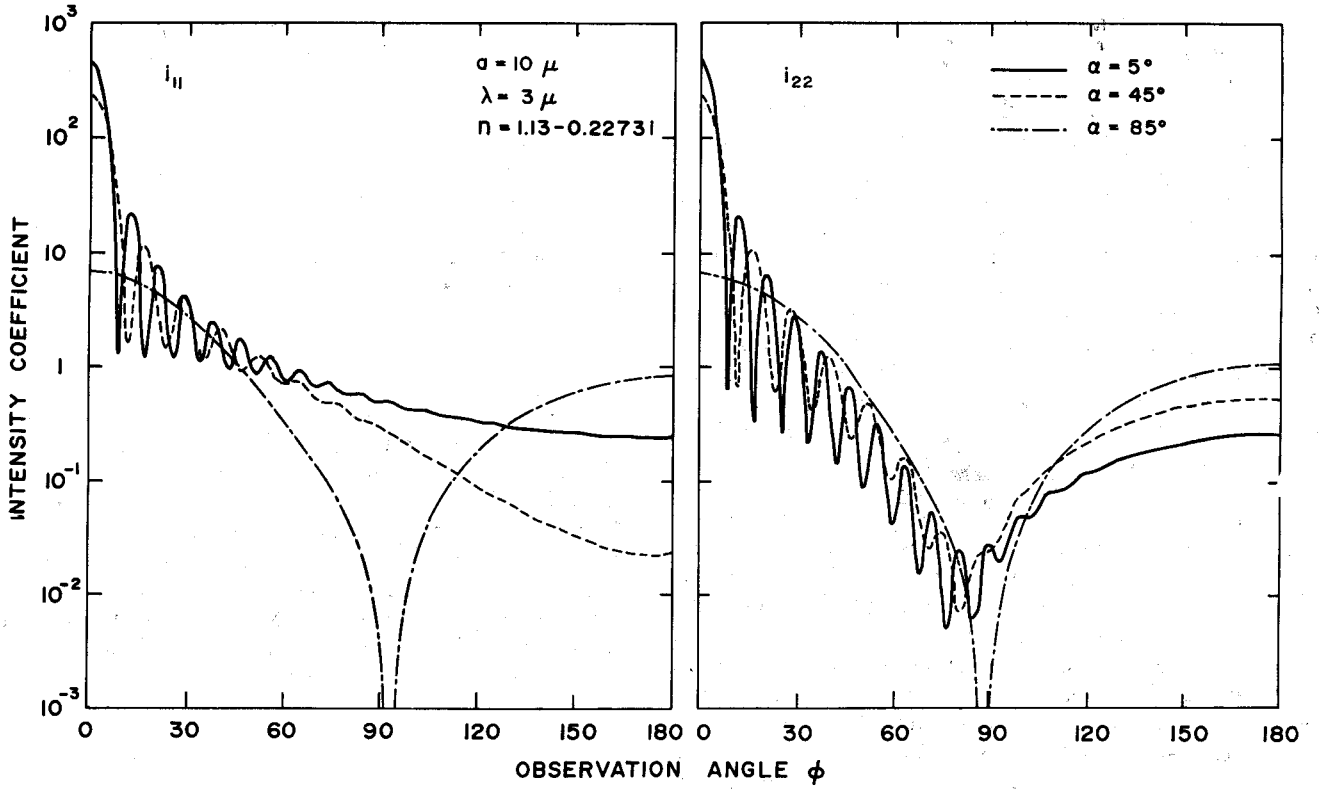

Fig. 5. Same as Fig. 4, but the incident wavelength λ is 3 μ.

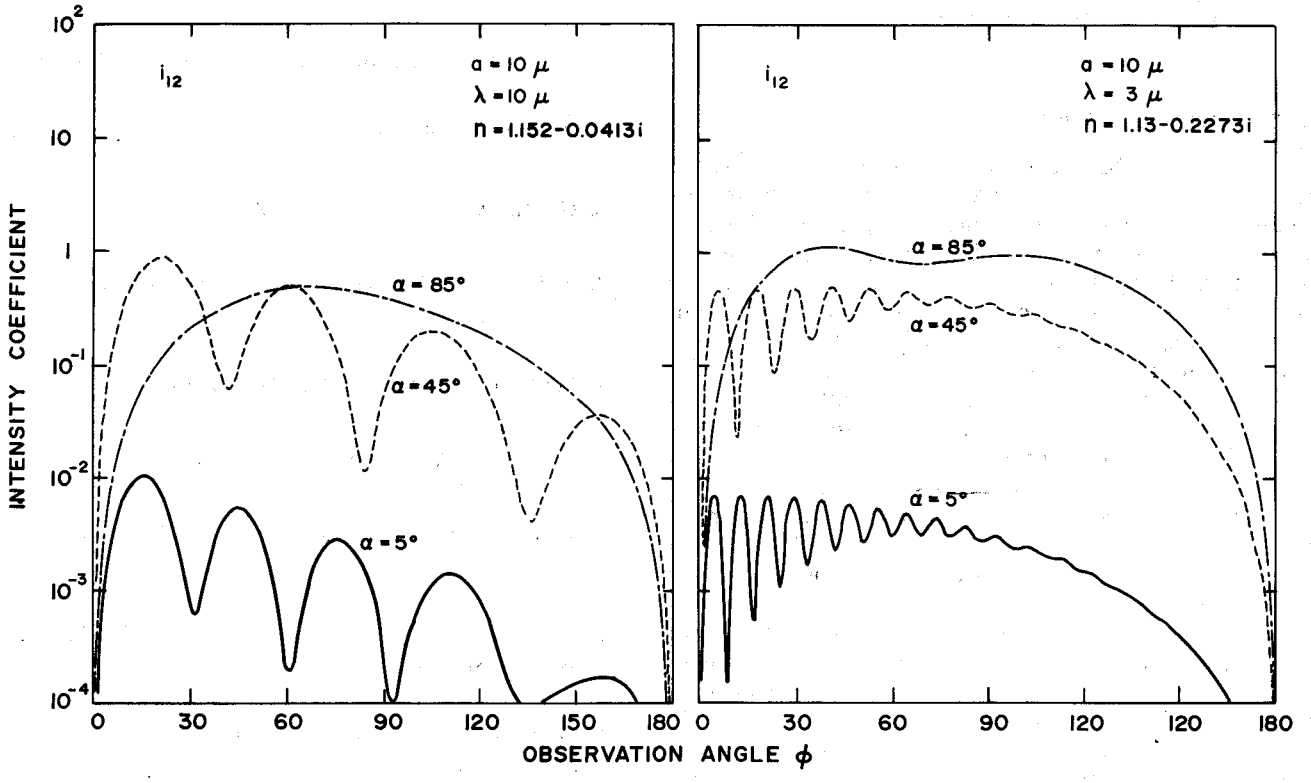

Fig. 6. The cross-polarized intensity coefficient i_{12} as a function of observation angle φ for light scattered by a cylinder of circular radius a of 10 μ with incident wavelengths λ of 10 μ (left-hand side) and 3 μ (right-hand side).

and their values are very similar. This means that scattering of light for a large oblique incident angle has no preference for the state of polarization of the incident energy. A minimum at the observation angle of 90° and two maxima with values near unity at $\phi = 0°$ and 180° are shown.

Figure 5 represents the intensity coefficients i_{11} and i_{22} for a cylinder of circular radius of 10 μ with an incident wavelength of 3 μ, which corresponds to a size parameter of 20.94. The refractive index for ice at 3 μ is 1.13 and 0.2273 for the real and imaginary parts, respectively. The absorption component is quite large. As a result, the rays refracted into or internally reflected in the cylinder are mostly absorbed. We can see that at observation angles larger than about 80°, almost no fluctuation occurs because the source of the scattered light comes primarily from the rays which undergo external reflection only. The maxima and minima shown near the smaller observation angles are mainly caused by rays that pass by the cylinder and form a diffraction pattern. Once again, for α of 85°, two similar and nearly symmetrical patterns for values of i_{11} and i_{22} are obtained. The values of i_{11} and i_{22} in Fig. 5 are in general greater than those in Fig. 4 because the size parameter in the former is about three times larger.

The cross-polarized intensity coefficient i_{12} for the above two cases is shown in Fig. 6. Their values seem to increase as the oblique incident angle increases, as can be easily observed in this figure. When $\alpha = 85°$, the maximum value for i_{12} is about unity in both cases. The zero values at observation angles of 0° and 180° again indicate that the scattered light retains the state of polarization of the incident energy.

Concluding Remarks

A solution for the scattering of electromagnetic waves by arbitrarily oriented, long cylinders, which are assumed to be homogeneous and isotropic but otherwise arbitrary, has been given. The scattering coefficients are obtained from boundary conditions and are suitable for computer calculations. Values of far-field intensities are expressed in a spherical coordinate system. The scattered light is shown to be confined to a solid cone the size of which depends on the oblique incident angle. For light that is not at normal incidence, there is no direct backscattering.

We have made light-scattering calculations for ice cylinders at three different incident wavelengths: 0.7 μ, 3 μ, and 10 μ. A strong diffraction pattern at the very forward direction for scattered intensities, which retain the same state of polarization as the incident intensities, is obtained. This diffraction component strongly depends on the size parameter. Moreover, the results show a very significant cross-polarized intensity for light obliquely incident on the cylinder. This cross-component disappears at normal incidence, which is similar to the case of scattering from a spherical particle. This is due to the fact that the cylinder is symmetrical with respect to the incident light.

The fluctuations of the scattered intensities due to single-particle effects increase with increasing size parameter, but decrease with increasing oblique incident angle. The scattering patterns become rather simple and symmetrical for light incident nearly parallel to the axis of the cylinder. Thus, one application of this result can be achieved by observing the scattering pattern at a sufficiently large oblique incident angle, so that the size of the cylinders may be determined with less fluctuated data.

I would like to thank D. K. Sze for his assistance in numerical programming, and J. W. Hovenier and J. E. Hansen for some discussions. Frequent discussions with R. M. Schotland on the problems of scattering from nonspherical particles and his encouragement are gratefully appreciated. During the course of this research, I held a NAS-NRC Postdoctoral Research Associateship supported by NASA. I would also like to thank the Director of the Institute, R. Jastrow, for providing the excellent research facilities.

References

1. D. Deirmendjian, Appl. Opt. **3**, 187 (1964).
2. J. V. Dave, Appl. Opt. **8**, 155 (1969).
3. J. E. Hansen and J. B. Pollack, J. Atmos. Sci. **27**, 265 (1970).
4. K. N. Liou and J. E. Hansen, J. Atmos. Sci. **28**, 995 (1971).
5. G. Mie, Ann. Phys. **25**, 377 (1908).
6. B. J. Mason, *Physics of Clouds* (Oxford U.P., London, 1957), p. 481.
7. Lord Rayleigh, Philos. Mag. **36**, 365 (1918).
8. J. R. Wait, Can. J. Phys. **33**, 189 (1955).
9. J. A. Stratton, *Electromagnetic Theory* (McGraw-Hill, New York, 1941), p. 415.
10. H. C. van de Hulst, *Light Scattering by Small Particles* (Wiley, New York, 1957), p. 452.
11. W. M. Irvine and J. B. Pollack, Icarus **8**, 324 (1968).
12. M. Abramowitz and I. A. Stegun, *Handbook of Mathematical Functions* (Dover, New York, 1965), p. 1046.